Supporting Information

Room-temperature quasi-catalytic hydrogen generation from waste and water

Hongguo Wu [a], Li-Long Zhang [a], Junqi Wang [b], Yiyuan Jiang [a], Hu Li [a,*], Putla Sudarsanam [c,*], Song Yang [a,*]

[a] State Key Laboratory Breeding Base of Green Pesticide & Agricultural Bioengineering, Key Laboratory of Green Pesticide & Agricultural Bioengineering, Ministry of Education, State-Local Joint Laboratory for Comprehensive Utilization of Biomass, Center for R&D of Fine Chemicals, Guizhou University, Guiyang, Guizhou, 550025, China

[b] Department of Earth and Environmental Science, School of Human Settlements and Civil Engineering, Xi'an Jiaotong University, Xi'an, Shaanxi, 710049, China

[c] Catalysis and Inorganic Chemistry Division, CSIR-National Chemical Laboratory, Dr Homi Bhabha Road, Pashan, Pune 411008, India

This supplementary information file includes:

- Supplementary Notes 1–6
- Supplementary Tables 1–8
- Supplementary Figures 1–8
- Supplementary References 1–13

Supplementary Notes

1. Materials

Phenylsilane ($PhSiH_3$, 97%), dimethylphenylsilane ($PhMe_2SiH$, 97%), diphenylsilane (Ph_2SiH_2, 97%), polymethylhydrosiloxane (PMHS), triethoxysilane ($(EtO)_3SiH$, 97%), trimethoxysilane ($(MeO)_3SiH$, 95%), trimethoxyphenylsilane ($PhSiO(CH_3)_3$, 98%), triethylsilane (Et_3SiH, 98%), 1,1,1,3,5,5,5-heptamethyltrisiloxane ($(Me_3SiO)_2MeSiH$, 98%), 1,1,3,3-tetramethyldisiloxane ($(Me_2SiH)_2O$, 98%), propylene carbonate (PPC, 99.7%), *γ*-valerolactone (GVL, 98%), methanol-d_4 (99.8 atom% D), 2-methyltetrahydrofuran (2-MeTHF, ≥99.5%), *N,N'*-dimethyl-propylene-urea (DMPU, 99%), *N,N'*-dimethylformamide (DMF, 99%), and 2-butanol (99.5%) were purchased from Shanghai Aladdin Industrial Inc. Dimethyl sulfoxide (DMSO, 99.9%), methanol (MeOH, ≥99.9%), acetonitrile (MeCN, ≥99.0%), tetrahydrofuran (THF, ≥99.9%), ethanol (99.9%), 1-hexanol (99%), isopropanol (99.9%), 1,4-butanediol (99%), 1,5-pentanediol (98%), poly(ethylene glycol) (Mn 600), and glycerol (99.5%) were purchased from Beijing Innochem Inc.

2. Reaction procedures

All the experiments were conducted in a double-walled thermostatically controlled reaction vessel with a reflux condenser, which was connected to an automatic gas burette, where the gases were collected. In a general procedure, 1 mmol hydrosilane was added into the reaction vessel at 25-80 °C, and subsequently, the reaction was started by the addition of 1 mL DMPU/alcohol (5:5, v/v) or DMPU/H_2O (8:2, v/v). During this reaction, the evolved gas was qualitatively and quantitatively analyzed by an Agilent 6820 GC equipped with a TDX-01 column connected to a thermal conductivity detector (TCD).

3. Analysis of products

Quantitative analyses of the reaction mixtures were conducted by a GC (Agilent

7890B) with an HP-5 column (30 m × 0.320 mm × 0.25 μm) and a flame ionization detector (FID) using naphthalene as an internal standard. GC-MS (Agilent 6890N GC/5973 MS, Santa Clara, CA) was used to identify products, intermediates, and major by-products. In addition, ^{1}H NMR was also used for the quantification of unpurified products in the reaction mixtures (diluted with $CDCl_3$) using 1,3,5-trimethoxybenzene as the internal standard. With respect to isotopic labeling experiments, GC-MS spectra for some of the liquid mixtures were measured to determine the incorporated D in the product.

4. Theoretical computation

All structure optimization and quantum chemistry calculations were performed using Gaussian 09 software package [S1]. Geometry optimization and frequency calculations were calculated at ambient pressure and temperature of 303 K with density functional theory (DFT) at the WB97XD/6-311G(d,p) level of theory [S2]. In this work, all atoms were fully relaxed during geometrical optimization. To get more precise electronic energies, single-point calculations were carried out on the optimized geometries using B2PLYPD3/DEF2TZVP [S3]. The bulk solvent effect of DMPU media can be considered by the self-consistent reaction field (SCRF) technique. The solvation energies were obtained at the level of M05-2X/6-31G(d) [S4] with the solvation model density (SMD) solvent model.

5. Life cycle assessment (LCA)

In this study, LCA was conducted using CML baseline to better understand and compare the impact categories. The framework, principles, and guidelines for LCA were followed as described within the International Organization for Standardization standards, ISO 14040 and ISO 14044. Herein, the environmental LCA adopted the widely utilized Simapro v.8.0 LCA software. According to this method, five baseline impact indicators were assessed, including acidification potential, global warming potential, abiotic depletion potential, eutrophication potential, and ozone layer depletion.

The goal of this study was to compare the environmental impact of H_2 production from industrial and our developed method. The environmental footprints of all input processes of the entire life cycle from H_2 production to by-product recovery were included in this study. The detailed process in the information was obtained from the lab working, and the data for LCA were mainly retrieved from the Ecoinvent database v3.6. The functional unit (FU) used in this work was 1 kg of H_2.

6. Molecular dynamics simulations

Molecular dynamics (MD) simulations were performed to study the DMPU, CH_3OH and $PhSiH_3$ behavior [S5]. Our simulation calculation was conducted on four structures with an integration time-step of 1 fs. Periodic boundary conditions were applied in the *x*- and *y*-dimensions. The box size of the samples was 17 × 17 × 17 nm^3. First, the conjugate gradient algorithm and energy minimization were performed to obtain a stable structure. Condensed-phased Optimized Molecular Potential for Atomistic Simulation Studies force field was also used to optimize these structures in the Materials studio with Forcite Module. Each sample was then equilibrated under the NPT ensemble at a constant temperature of 300 K to achieve an equilibrium state with zero pressure for 30 ns. The equilibration molecular systems of the pure separation membrane could be obtained after geometrically optimizing. One system of separation is composed of 30 DMPU, 30 CH_3OH, and $PhSiH_3$. Furthermore, a potential cutoff radius of 2.25 nm is applied in the calculation of the non-bonded interaction. And the particle-particle particle-mesh (PPPM) has been used to describe the electrostatic interaction. The Andersen feedback thermostat and Berendsen barostat algorithm are applied in the system with temperature and pressure conversion. Finally, the properties of our structures are obtained in the last 3000 ps. The radial distribution functions (RDFs), $g(r)$, give the probability of molecules occurring at the distance (r).

Supplementary Tables

Table S1. The effect of different mixture solvents on H_2 generation from $PhSiH_3$ and CH_3OH

$$PhSiH_3 + CH_3OH \xrightarrow{\text{Solvent}} H_2 + PhSi(OCH_3)_3$$

Entry	Solvent	Basicity (β)[S6-S9]	Polarity (π^*)[S6-S9]	Time (min)[a]	H_2 yield (%)	Rate (μmol/min)[b]
1	--	0.66	0.58	120	27	107
2	MeCN	0.4	0.75	30	23	147
3	2-MeTHF	0.58	0.53	40	16	167
4	THF	0.55	0.58	60	47	126
5	PPC	0.4	0.83	45	50	155
6	GVL	0.6	0.83	50	48	120
7	DMSO	0.76	1.00	40	6	54
8	DMF	0.69	0.88	60	75	51
9	DMPU	0.90	0.92	5	>99	1215

Reaction conditions: 1 mmol $PhSiH_3$, 1 mL methanol/solvent (5:5, v/v), and 25 °C

[a] The reaction time was recorded until almost no hydrogen was generated

[b] The reaction rate was determined in 2 min

Table S2. The deviation with $\nu_{Si\text{-}H}$ and $\nu_{O\text{-}H}$ in FT-IR-ATR spectra of different conditions [a]

Solvent	$\nu_{Si\text{-}H}$ /cm^{-1}	Deviation 1	$\nu_{Si\text{-}H}$ /cm^{-1}	Deviation 2	$\nu_{O\text{-}H}$ /cm^{-1}	Deviation 3
MeCN	2157.99	5.79	2157.99	1.93	3421.16	111.86
2-MeTHF	2154.13	1.93	2154.13	-1.93	3419.23	109.93
THF	2154.13	1.93	2154.13	-1.93	3421.16	111.86
PPC	2157.99	5.79	2157.99	1.93	3423.08	113.78
GVL	2156.06	3.86	2154.13	-1.93	3419.23	109.93
DMSO	2156.06	3.86	2156.06	0	3392.23	82.93
DMF	2154.13	1.93	2156.06	0	3394.16	84.86
DMPU	2153.1	0.9	2153.1	-2.96	3382.59	73.29

[a] Different mixture solvents of FTIR spectra in $\nu_{Si\text{-}H}$ and $\nu_{O\text{-}H}$ region during the reaction of $PhSiH_3$ (0.1 mmol) with 0.1 mL methanol or methanol/solvent (5:5, v/v).

Deviation 1 = $\nu_{Si\text{-}H}$ of $PhSiH_3$ (2152.2 cm^{-1}) - $\nu_{Si\text{-}H}$ of $PhSiH_3$ in different solvents

Deviation 2 = $\nu_{Si\text{-}H}$ of $PhSiH_3$ in methanol (2156.06 cm^{-1}) - $\nu_{Si\text{-}H}$ of $PhSiH_3$ in different solvents with methanol

Deviation 3 = $\nu_{O\text{-}H}$ of MeOH with $PhSiH_3$ (3309.3 cm^{-1}) - $\nu_{O\text{-}H}$ of MeOH with $PhSiH_3$ in different solvents with methanol

Table S3. The effect of different solvent ratios on the H_2 production

Entry	Solvent	Time (min)[a]	H_2 Yield (%)	Rate (μmol/min)[b]
1	MeOH:DMPU = 8:2	10	>99	1140
2	MeOH:DMPU = 7:3	7	>99	1170
3	MeOH:DMPU = 6:4	6	>99	1185
4	MeOH:DMPU = 5:5	5	>99	1215
5	MeOH:DMPU = 4:6	5.5	>99	1200
6	MeOH:DMPU = 3:7	6	>99	1095
7	MeOH:DMPU = 2:8	7.5	>99	870

Reaction conditions: 1 mmol $PhSiH_3$, 1 mL solvent, and 25 °C.

[a] The reaction time was recorded until almost no hydrogen was generated

[b] The reaction rate was determined in 2 min

Table S4. The effect of different hydrosilanes on the production of H_2

$$R_{4-n}SiH_n + CH_3OH \xrightarrow{DMPU} H_2 + R_{4-n}Si(OCH_3)_n$$

Entry	Hydrosilane	Abbreviation	Temp (°C)	Time (min)[a]	H_2 yield (%)	Rate (μmol/min)[b]
1	Phenylsilane	$PhSiH_3$	25	5	>99	1215
2	Triethoxysilane	$(EtO)_3SiH$	25	25	>99	177
3	Diphenylsilane	Ph_2SiH_2	25	30	96	115
4	Polymethylhydrosiloxane	PMHS	25	30	98	140
5	Trimethoxysilane	$(MeO)_3SiH$	25	27	85	41
6	Dimethylphenylsilane	$PhMe_2SiH$	60	25	70	130
7	Triethylsilane	Et_3SiH	60	25	50	76
8	1,1,1,3,5,5,5-Heptamethyltrisiloxane	$(Me_3SiO)_2MeSiH$	60	30	50	81
9	1,1,3,3-Tetramethyldisiloxane	$(Me_2SiH)_2O$	60	25	35	94

Reaction conditions: 1 mmol hydrosilane and 1 mL methanol/solvent (5:5, v/v).

[a] The reaction time was recorded until almost no hydrogen was generated

[b] The reaction rate was determined in 2 min

Table S5. The effect of different alcohols on the production of H_2

$$PhSiH_3 + n\,R'OH \xrightarrow{DMPU} H_2 + PhSi(OR')_n$$

Entry	Alcohol: DMPU (5:5, v/v)	Acidity (α)	Basicity (β)	Polarity (π*)	Temp (°C)	Time (min)[a]	H_2 yield (%)	Rate (μmol/min)[b]
1	Methanol	0.93	0.66	0.58	25	5	>99	1215
2	Ethanol	0.83	0.75	0.51	25	30	92	165
3	1-Hexanol	0.80	0.84	0.40	25	30	79	45
4	Isopropanol	0.76	0.84	0.48	40	40	66	27
5	Isopropanol	0.76	0.84	0.48	60	40	84	99
6	2-Butanol	0.69	0.80	0.40	40	40	63	23
7	2-Butanol	0.69	0.80	0.40	60	27	83	84
8	Ethylene glycol	0.90	0.52	0.92	25	15	91	630
9	1,4-Butanediol	0.78	0.54	0.87	25	20	97	270
10	1,5-Pentanediol	-	-	-	25	25	88	240
11	Glycerol	0.93	0.67	1.04	25	60	80	135
12	Poly(ethylene glycol)	0.32	0.66	0.84	25	25	97	225

Reaction conditions: 1 mmol $PhSiH_3$, 1 mL solvent, and 25 °C

[a] The reaction time was recorded until almost no hydrogen was generated

[b] The reaction rate was determined in 2 min

Table S6. Bond dissociation energies (BDE) of some hydrosilanes

Entry	Hydrosilane	BDE Si-H (kJ mol^{-1}) [S10]
1	$PhSiH_3$	88.9
2	Ph_2SiH_2	89
3	$PhMe_2SiH$	91.3
4	Et_3SiH	92.8

Table S7. The effect of different ratios of H_2O/DMPU (v/v) on the production of H_2

$$PhSiH_3 + H_2O \xrightarrow{DMPU} H_2 + PhSi(OH)_3$$

Entry	Ratio of H_2O:DMPU (v/v)	Time[a] (min)	H_2 Yield (%)	Rate[b] (μmol/min)
1	10:0	150	62	15
2	8:2	25	87	120
3	7:3	20	90	300
4	6:4	18	91	330
5	5:5	15	91	360
6	4:6	14	92	405
7	3:7	6	>99	1410
8	2:8	5.5	>99	1485
9	1:8	5	>99	1436
10	1:10	4	>99	1425
11	1:20	5	>99	1205

Reaction conditions: 1 mmol $PhSiH_3$, 1 mL mixture solvent, and 25 °C

[a] The reaction time was recorded until almost no hydrogen was generated

[b] The reaction rate was determined in 2 min

Table S8. The effect of different hydrosilanes on the production of H_2 from H_2O

$$R_{4-n}SiH_n + H_2O \xrightarrow{DMPU} H_2 + R_{4-n}Si(OH)_n$$

Entry	Hydrosilane	Temp (°C)	Time (min)[a]	H_2 yield (%)	Rate (μmol/min)[b]
1	$PhSiH_3$	25	4	>99.9	1425
2	Ph_2SiH_2	25	10	>99.9	1365
3	$(EtO)_3SiH$	25	16	91	323
4	$(MeO)_3SiH$	25	10	87	319
5	PMHS	25	20	85	113
6	PMHS	30	9	96	1264
7	Pentasilane	30	5	>99	1372
8	Polyhydrosiloxane (PHS)	30	7	98	1316
9	$(Me_3SiO)_2MeSiH$	30	15	93	446
10	$(Me_2SiH)_2O$	30	15	91	425
11	Et_3SiH	30	6	82	971
12	$PhMe_2SiH$	30	10	80	650

Reaction conditions: 1 mmol hydrosilane and 1 mL H_2O-DMPU solvent (1:10, v/v)

[a] The reaction time was recorded until almost no hydrogen was generated

[b] The reaction rate was determined in 2 min

Note: Gel or colloidal compound was found in Entries 4-12, which may coat hydrosilane substrate to remarkably impede the reaction.

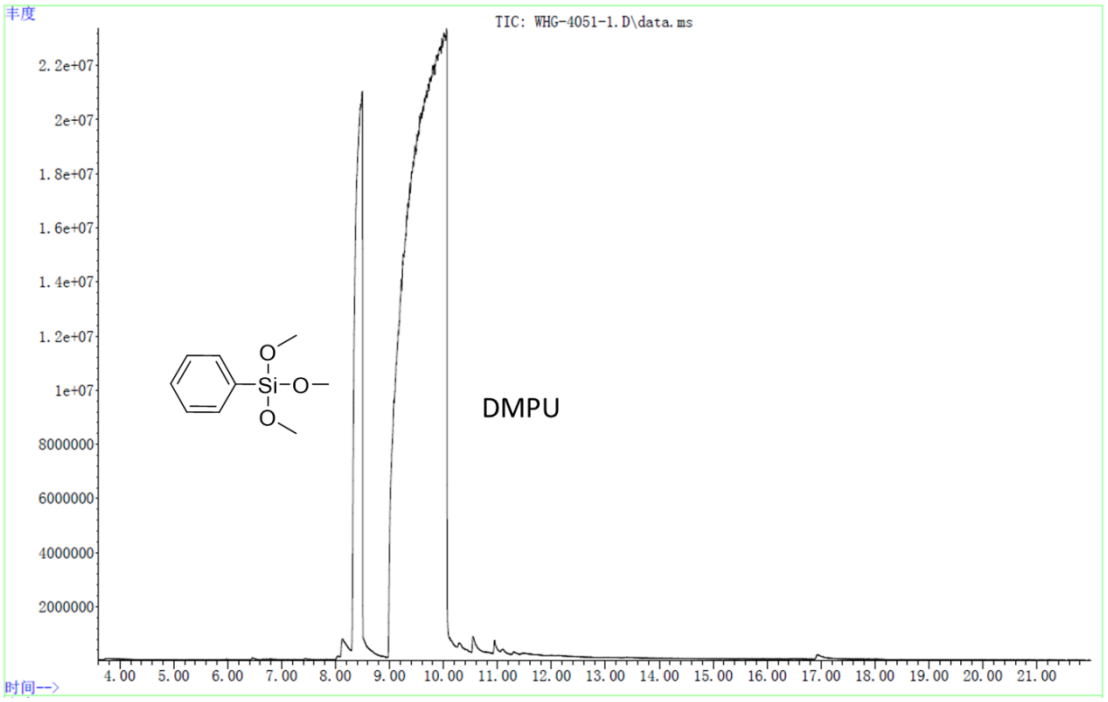

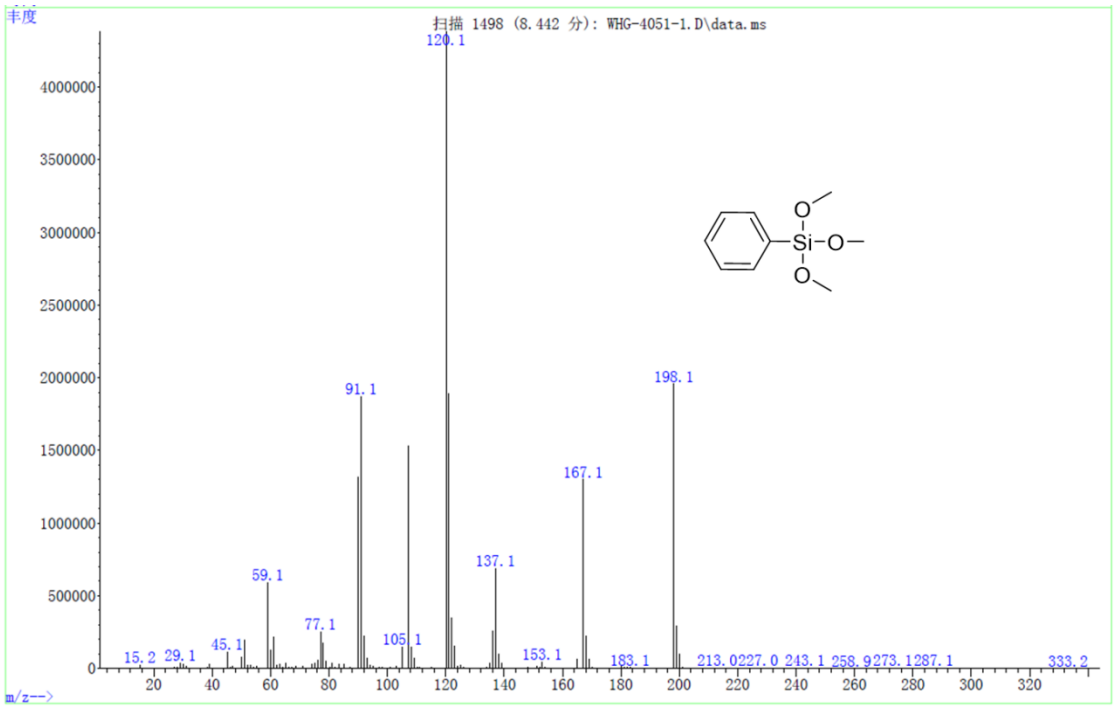

Figure S1 GC-MS spectrum of $PhSi(OCH_3)_3$.

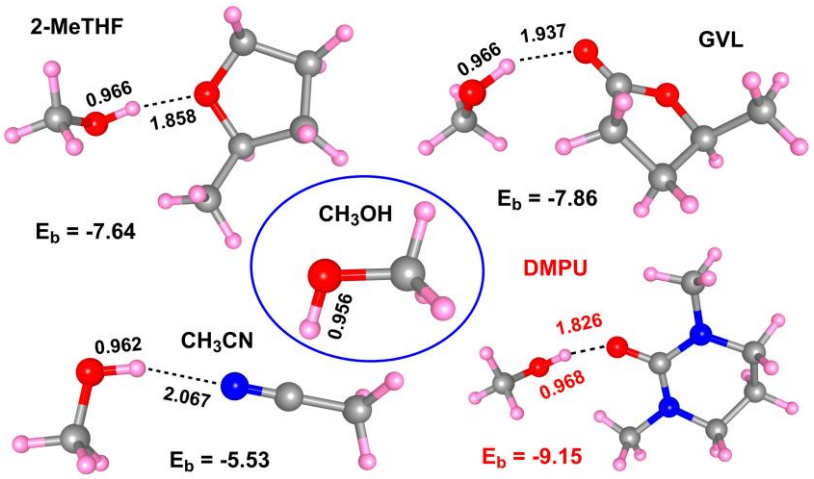

Figure S2. Calculated interaction model between methanol and organic solvents (E_b is binding energy, kcal mol^{-1})

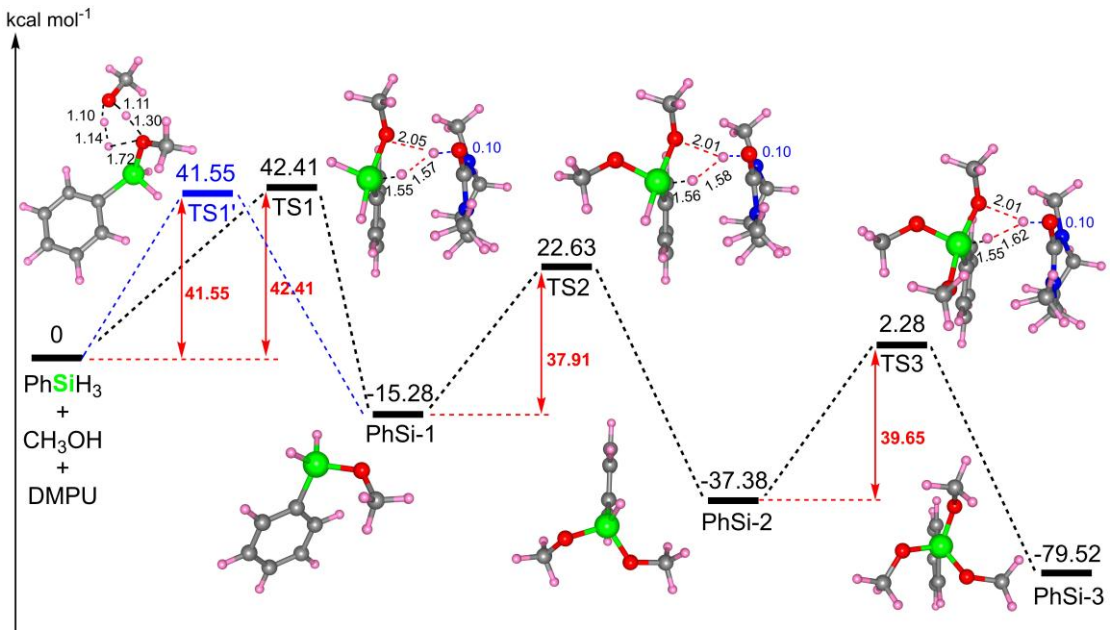

Figure S3. Computed free energy profiles for DMPU-enabled H_2 generation from $PhSiH_3$ and CH_3OH (TS: transition state)

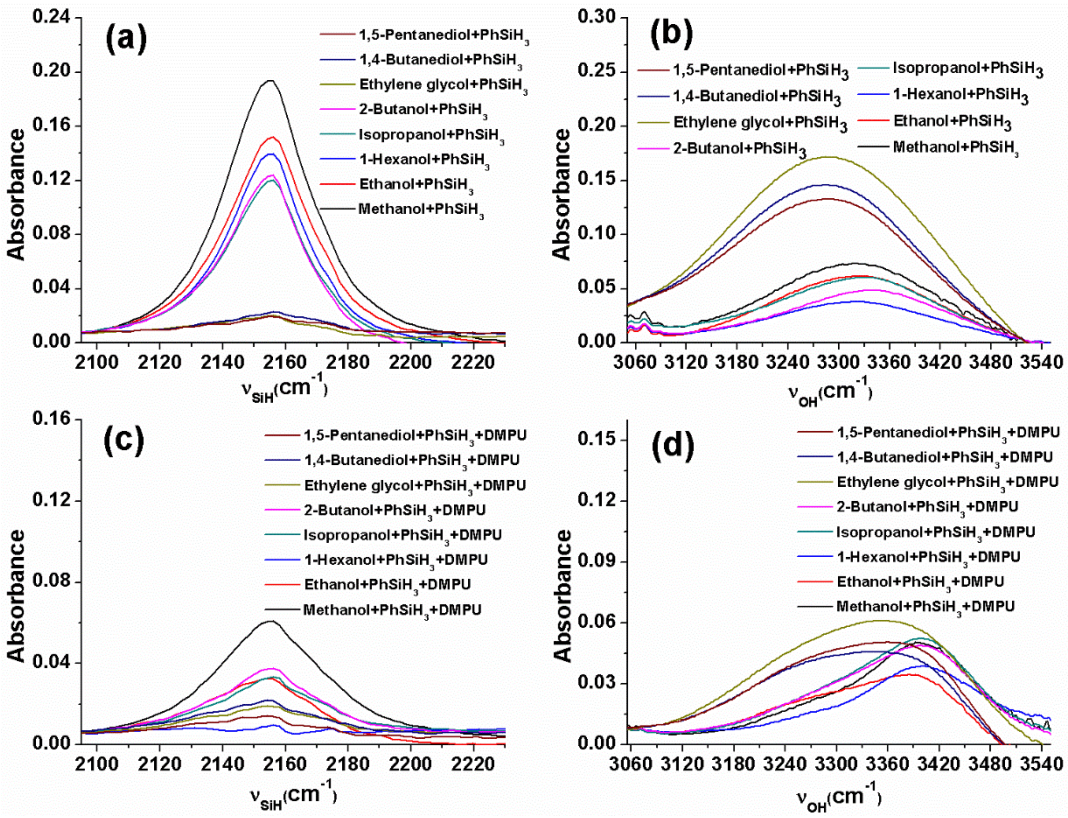

Figure S4. FT-IR-ATR spectra at (a), (c) ν_{SiH} and (b), (d) ν_{OH} regions for the reaction mixtures of $PhSiH_3$ (0.1 mmol) with 0.1 mL alcohol or alcohol-DMPU (5:5, v/v)

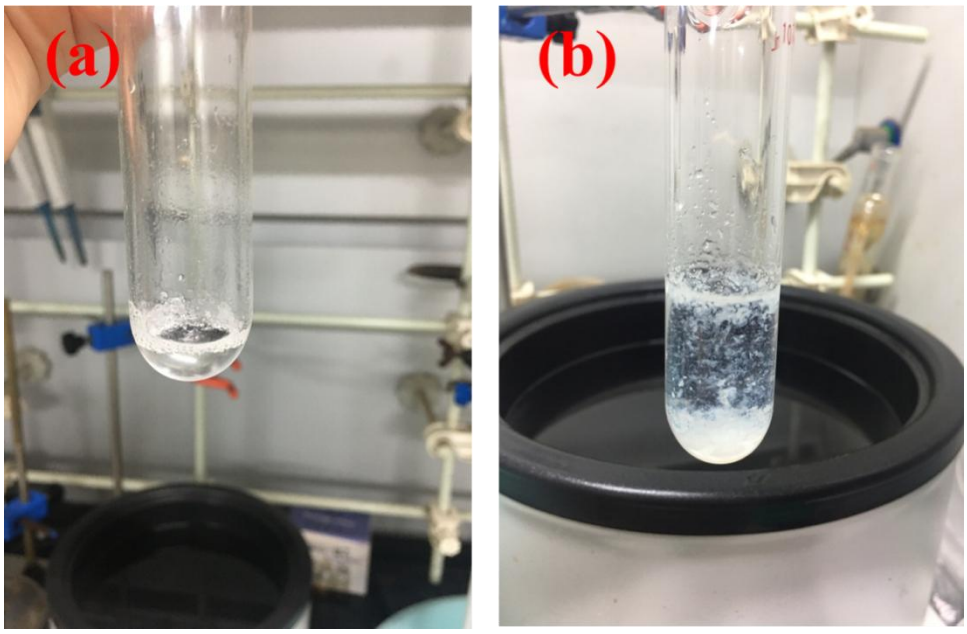

Figure S5. Images of reaction mixture before (**a**) and after (**b**) the reaction

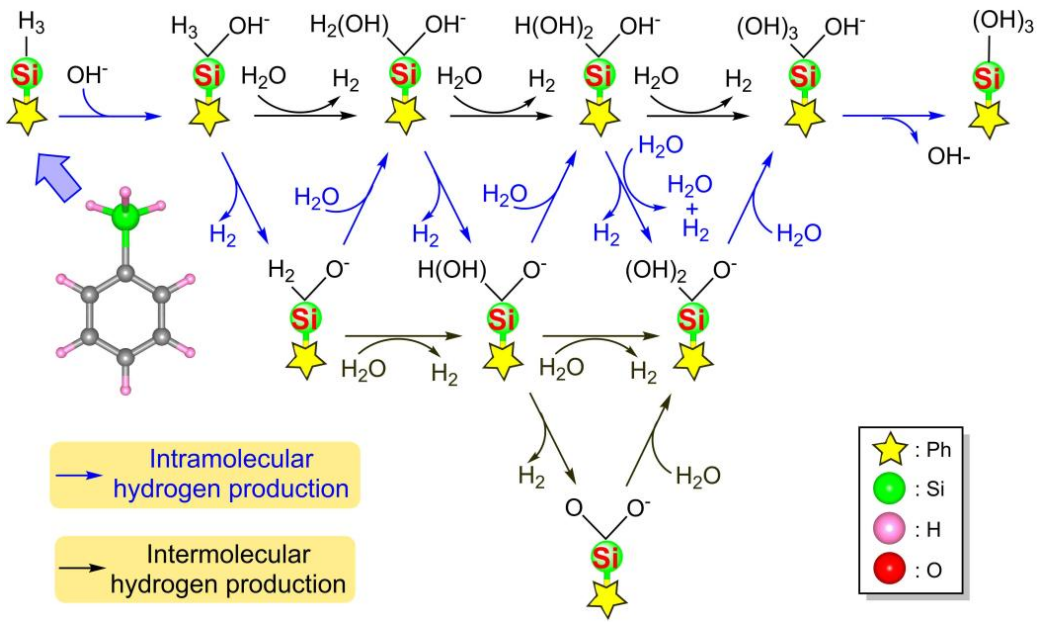

Figure S6. Schematic illustration for reaction pathways of H_2 generation from H_2O and $PhSiH_3$

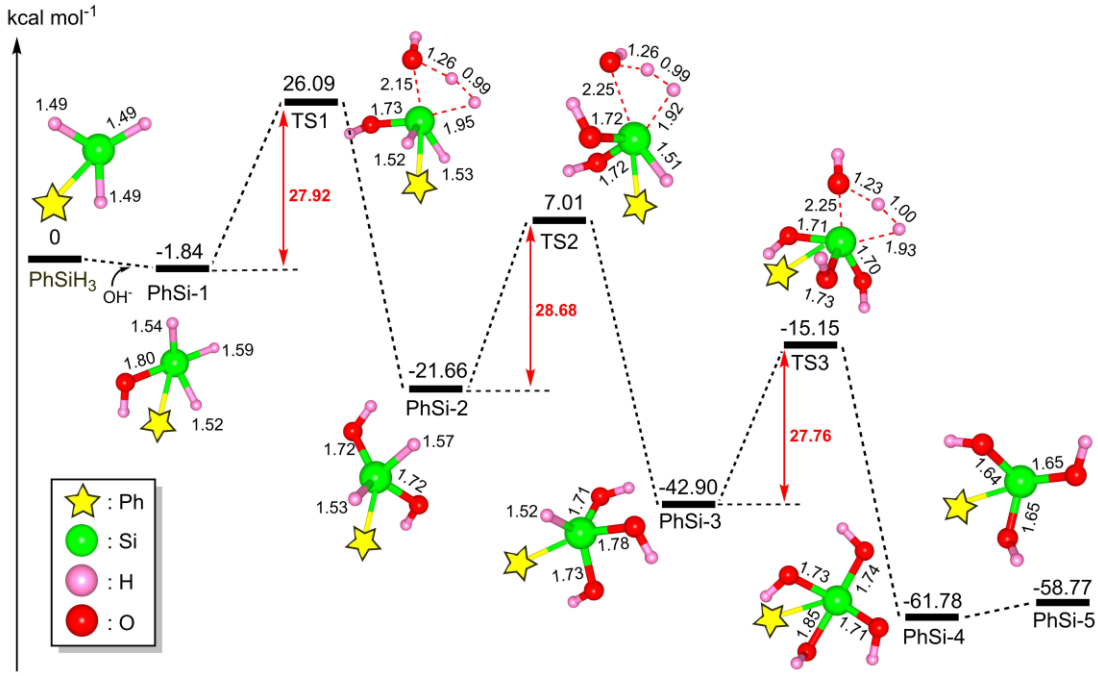

Figure S7. Computed free energy profiles for intermolecular H_2 production from $PhSiH_3$ and H_2O enabled by DMPU via penta-coordinated Si reaction pathway. (TS: transition state)

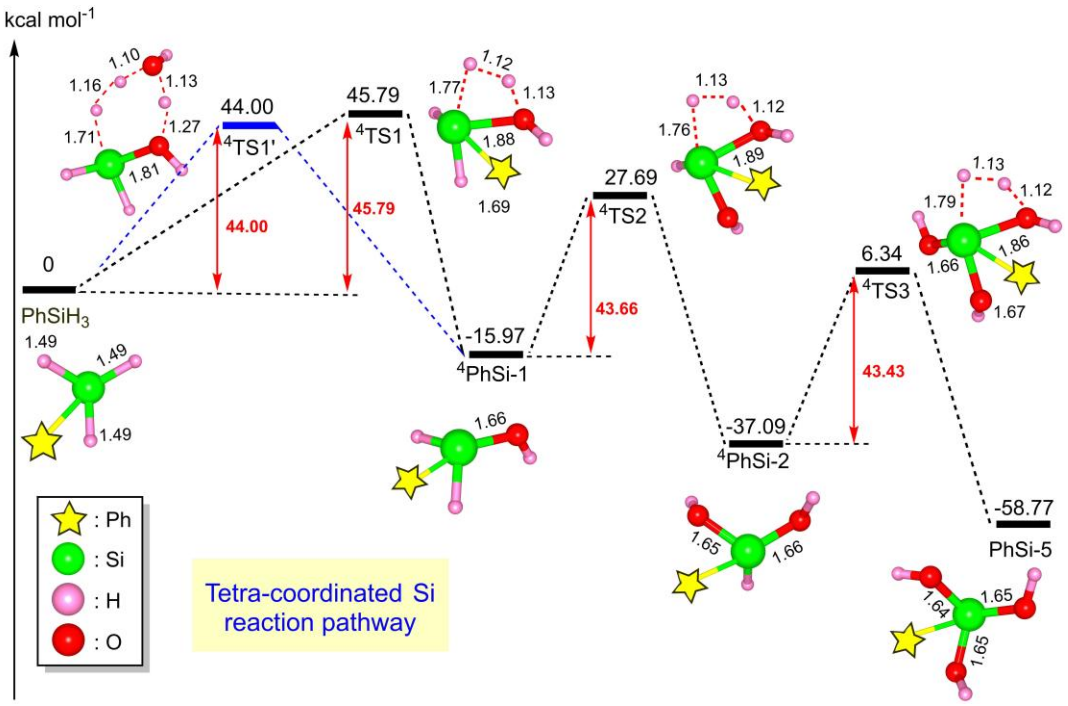

Figure S8. Computed free energy profiles for intermolecular H_2 production from $PhSiH_3$ and H_2O enabled by DMPU via tetra-coordinated Si reaction pathway. (TS: transition state)

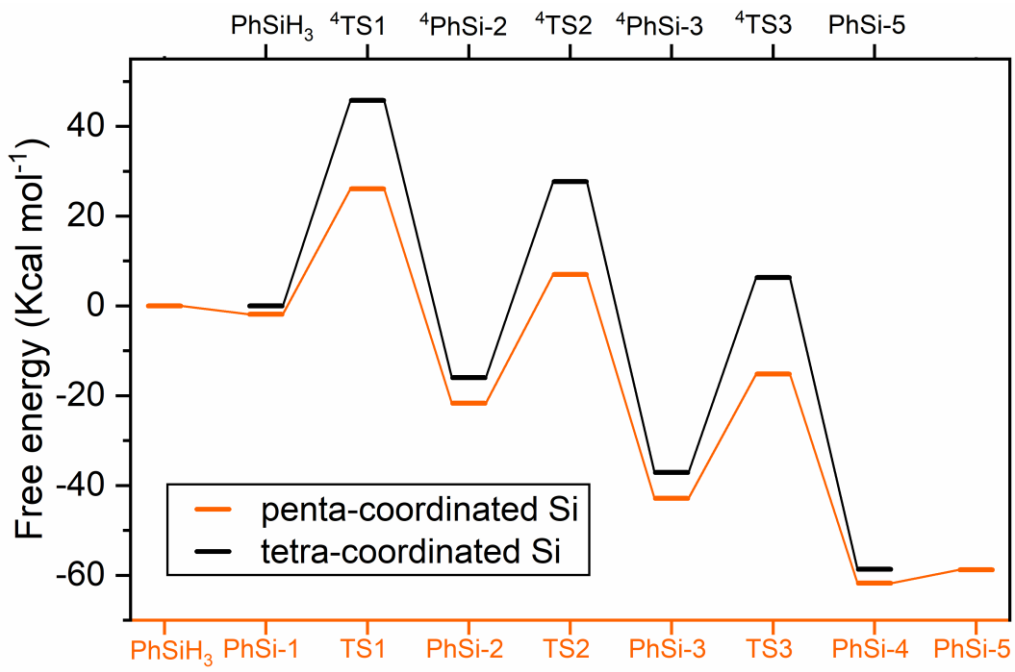

Figure S9. Comparison of computed free energy profiles for intermolecular H_2 production from $PhSiH_3$ and H_2O in DMPU via penta- and tetra-coordinated Si reaction pathway.

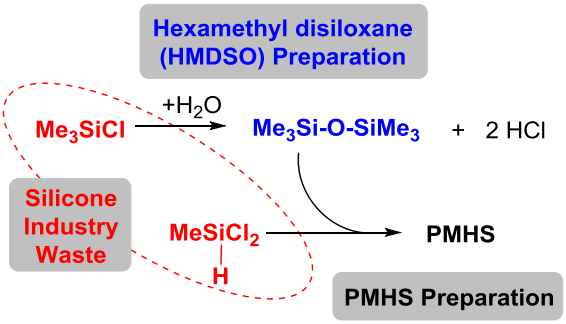

Figure S10. Schematic illustration of preparing PMHS from silicone industry waste
PMHS: polymethylhydrosiloxane

The relevant prepared procedures can be found in the references S11-S13.

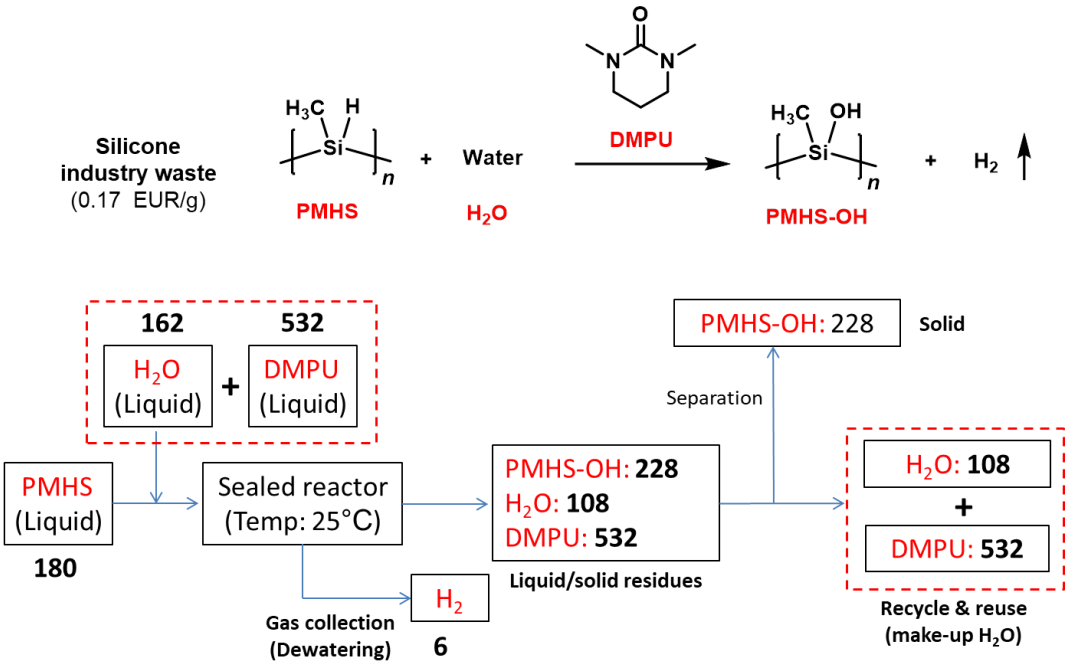

Figure S11. Process diagram of producing H_2 from PMHS and H_2O with DMPU
PMHS: polymethylhydrosiloxane

Supplementary References

S1. Frisch, M. J., Trucks, G. W., Schlegel, H. B., Scuseria, G. E., Robb, M. A., Cheeseman, J. R., Scalmani, G., Barone, V., Mennucci, B., Petersson, G. A., et al., *Gaussian 09*, Revision D.01; Gaussian, Inc.: Wallingford, CT, 2009.

S2. Chai, J. D., Head-Gordon, M. Long-range corrected hybrid density functionals with damped atom–atom dispersion corrections. *Phys. Chem. Chem. Phys.* **2008**, *10*, 6615-6620.

S3. Grimme, S., Antony, J., Ehrlich, S., Krieg, H. A consistent and accurate Ab initio parametrization of density functional dispersion correction (DFT-D) for the 94 elements H-Pu. *J. Chem. Phys.* **2010**, *132*, 154104.

S4. Zhao, Y., Schultz, N. E., Truhlar, D. G. Design of density functionals by combining the method of constraint satisfaction with parametrization for thermochemistry, thermochemical kinetics, and noncovalent interactions. *J. Chem. Theory Comput.* **2006**, *2*, 364-382.

S5. Jin, C., Xiang, N., Zhu, X., Shuang, E., Sheng, K., Zhang, X. Selective 5-hydroxymethylfurfural production from cellulose formate in DMSO-H_2O media. *Appl. Catal. B: Environ.* **2021**, *285*, 119799.

S6. Jessop, P. G., Jessop, D. A., Fu, D., Phan, L. Solvatochromic parameters for solvents of interest in green chemistry. *Green Chem.* **2012**, 14, 1245-1259.

S7. Mouret, A., Leclercq, L., Mühlbauer, A., Nardello-Rataj, V. Eco-friendly solvents and amphiphilic catalytic polyoxometalate nanoparticles: a winning combination for olefin epoxidation. *Green Chem.* **2014**, 16, 269-278.

S8. Smirnov, V. I., Badelin, V. G. Enthalpies of solution of *L*-phenylalanine in aqueous solution of amides at 298.15 K. *Thermochim. Acta* **2013**, 551, 145-148.

S9. Guo, H., Duereh, A., Su, Y., Hensen, E., Qi, X., Smith, R. L. Mechanistic role of protonated polar additives in ethanol for selective transformation of biomass-related compounds. *Appl. Catal. B: Environ.* **2020**, 264, 118509.

S10. Wang, H. J., Fu, Y. Designing new free-radical reducing reagents: Theoretical study on Si–H bond dissociation energies of organic silanes. *J. Mol. Struct. Theochem* **2009**, 893, 67-72.

S11. Brinson, J. A. *Recovery of Valuable Chlorosilane Intermediates by a Novel Waste Conversion Process*. United States, **2002**. DOI: 10.2172/795522.

S12. Noll, W. *Chemistry and technology of silicones*. Academic Press, New York, **1968**.

S13. Sauer, R. O., Scheiber, W. J., Brewer, S. D. Derivatives of the methylchlorosilanes. V. Polysiloxanes from methyldichlorosilane. *J. Am. Chem. Soc.*, **1946**, 68, 962-963.